ADVANCES IN ATMOSPHERIC SCIENCES, VOL. 29, NO. 2, 2012, 359–368

Reconstructed Light Extinction Coefficients Using Chemical Compositions of $PM_{2.5}$ in Winter in Urban Guangzhou, China

TAO Jun[1,2] (陶 俊), CAO Jun-Ji[3] (曹军骥), ZHANG Ren-Jian[4] (张仁健), ZHU Lihua[2] (朱李华), ZHANG Tao[2] (张 涛), SHI Si[1] (施 思), and CHAN Chuen-Yu*[1] (陈尊裕)

[1] *School of Environmental Science and Engineering of Sun Yat-Sen University, Guangzhou* 510275

[2] *South China Institute of Environmental Sciences, Guangzhou* 510655

[3] *Institute of Earth Environment, Chinese Academy of Sciences, Xi'an* 710075

[4] *Key Laboratory of Regional Climate-Environment for Temperate East Asia, Institute of Atmospheric Physics, Chinese Academy of Sciences, Beijing* 100029

(Received 16 April 2011; revised 23 July 2011)

ABSTRACT

The objective of this study was to reconstruct light extinction coefficients (b_{ext}) according to chemical composition components of particulate matter up to 2.5 μm in size ($PM_{2.5}$). $PM_{2.5}$ samples were collected at the monitoring station of the South China of Institute of Environmental Science (SCIES, Guangzhou, China) during January 2010, and the online absorbing and scattering coefficients were obtained using an aethalometer and a nephelometer. The measured values of light absorption coefficient by particle (b_{ap}) and light scattering coefficient by particle (b_{sp}) significantly correlated ($R^2 > 0.95$) with values of b_{ap} and b_{sp} that were reconstructed using the Interagency Monitoring of Protected Visual Environments (IMPROVE) formula when RH was <70%. The measured b_{ext} had a good correlation ($R^2 > 0.83$) with the calculated b_{ext} under ambient RH conditions. The result of source apportionment of b_{ext} showed that ammonium sulfate [$(NH_4)_2SO_4$] was the largest contributor (35.0%) to b_{ext}, followed by ammonium nitrate (NH_4NO_3, 22.9%), organic matter (16.1%), elemental carbon (11.8%), sea salt (4.7%), and nitrogen dioxide (NO_2, 9.6%). To improve visibility in Guangzhou, the effective control of secondary particles like sulfates, nitrates, and ammonia should be given more attention in urban environmental management.

Key words: light extinction coefficients, $PM_{2.5}$ aerosol, chemical species

Citation: Tao, J., J.-J. Cao, R.-J. Zhang, L. H. Zhu, T. Zhang, S. Shi, and C.-Y. Chan, 2012: Reconstructed light extinction coefficients using chemical compositions of $PM_{2.5}$ in winter in urban Guangzhou, China. *Adv. Atmos. Sci.*, **29**(2), 359–368, doi: 10.1007/s00376-011-1045-0.

1. Introduction

Visibility degradation is a prevalent phenomenon due to the high concentration of air pollutants in many megacities across China (Wu et al., 2005 Cheung et al., 2005; Yang et al., 2007; Deng et al., 2008; Tan et al., 2009). The major cause of visibility impairment or haze is light scattering and absorption by fine particles in the atmosphere (Watson, 2002). Although the extinction of visible light from gaseous species can also impair visibility, these species have a weak influence (Chan et al., 1999). Previous studies have shown that sulfates and element carbon in fine particles are the main chemical species that contribute to visibility degradation through scattering and absorption, respectively (Malm et al., 1994; Cheung et al., 2005; Cheng et al., 2008; Tao et al., 2009). Moreover, meteorological factors, especially relative humidity (RH), also contribute to the degradation of visibility (Malm and Day, 2001; Liu et al., 2008).

*Corresponding author: CHAN Chuen-Yu, chzy@mail.sysu.edu.cn

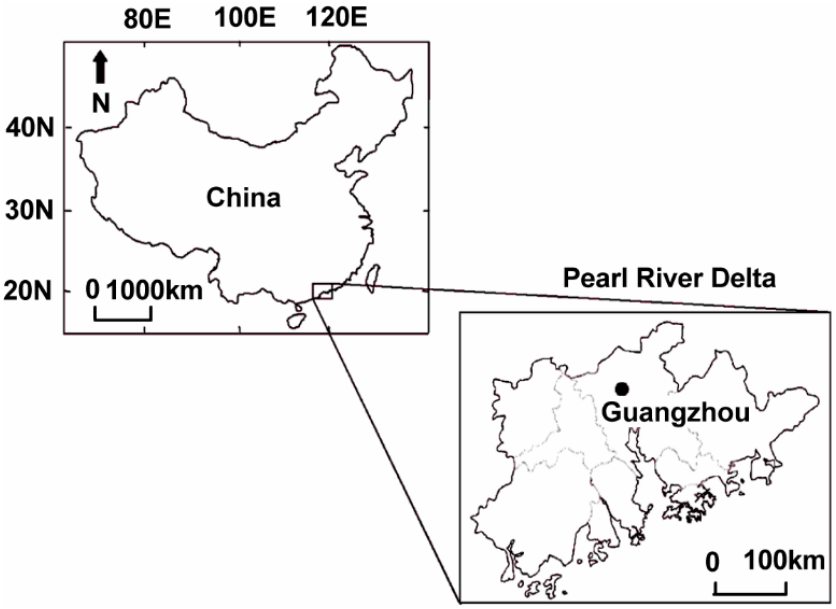

Fig. 1. Sampling location in Guangzhou.

The light extinction coefficient of particles can be expressed by light scattering and light absorption by particles. The light extinction coefficient can be obtained directly using a nephelometer and an aethalometer. An empirical formula relating light extinction coefficient and chemical species of particulate matter up to 2.5 μm in size ($PM_{2.5}$) has been established by the Interagency Monitoring of Protected Visual Environments (IMPROVE) network. The empirical formula used by IMPROVE has been used in some megacities in China for source apportionment of visibility degradation (Cheung et al., 2005; Yang et al., 2007; Tao et al., 2009). But few studies have compared the light extinction coefficient measured by nephelometer and aethalometer with those calculated using the IMPROVE empirical formula in China (Jung et al., 2009).

In this study, light scattering and absorption coefficients measured using nephelometer and aethalometer and chemical composition of $PM_{2.5}$ were determined for the 2010 winter period (from 1 January to 31 January 2010). The objective of this study was to reconstruct light scattering and absorption coefficients of particles and to compare them using the IMPROVE formula, then to investigate the contribution of chemical species of $PM_{2.5}$ to visibility impairment in Guangzhou. Control of the largest contributors can then be a focus of urban environmental management.

2. Methodology

2.1 *Site description*

The monitoring station of the South China of Institute of Environmental Science (SCIES) is located at the urban area of Guangzhou (23°07′N, 113°21′E; see Fig. 1). No obvious industrial pollution source is present near the monitoring station. The instruments used in this study were installed on the roof (50 m above ground) of a building in the SCIES complex. The Guangzhou observation station is a supersite designed to monitor measure $PM_{2.5}$ mass, the major chemical components of PM (sulfate, nitrate, ammonium, organic material, elemental carbon, and crustal related material), aerosol optical properties (aerosol optical depth, absorption coefficient, and scattering coefficient), atmospheric pollutants (e.g., ozone, CO, SO_2, NO_x), and meteorology parameters (wind, temperature, pressure, and relative humidity) with many new measurement technologies. The goals of the Guangzhou supersite are twofold: first, to provide a platform for routine PM and gas-phase measurement methods, and second, to provide data to advance our scientific understanding of atmospheric processes of air pollution in Guangzhou.

2.2 *Continuous observation of scattering and absorbing coefficients of aerosol*

Scattering coefficients (b_{sp}) of aerosol were measured using an integrating nephelometer (TSI Incorporated, Shoreview, MN, U.S.A., Model 3563) in three wavelengths: 450 nm, 550 nm, and 700 nm. Calibration of the nephelometer was performed using carbon dioxide (CO_2) as high-span gas and filtered air as low-span gas. This instrument draws the ambient air through a temperature-controlled inlet at a flow rate of 20 L min^{-1}. The heater in the nephelometer controls the RH of the aerosol intake at a level of <70%.

The data averaging time was 1 min. The baseline (zero level) data was measured continuously for 5 min after each hourly (60-min) sample. This study used 550-nm data.

Absorbing coefficients of 532 nm (b_{ap}) were converted to concentrations in μg m^{-3} using an equivalency of 8.28 m^2 g^{-1} when λ = 880 nm (Yan et al., 2008; Wu et al., 2009) using an aethalometer (Magee Scientific Company, Berkeley, CA, U.S.A., Model AE-31). The flow rate of the aethalometer was 5 L min^{-1}. The aethalometer was calibrated to zero by replacing the filter in the canister inlet with a clean filter every week.

2.3 *$PM_{2.5}$ sample collection and analysis*

The $PM_{2.5}$ samples were collected using an air sampler (BGI Incorporated, Waltham, MA, U.S.A., Model PQ200). This sampler was equipped with a cyclone that separates the particles with an aerodynamic diameter <2.5 μm when a vacuum pump draws air at a rate of 16.7 L min^{-1}. The airstream was connected to the 47-mm quartz filter (Whatman International Ltd, Maidstone, England, QMA). Before sampling, the quartz filters were baked at 800°C for $\geqslant$3 h to remove adsorbed organic vapors and then were equilibrated in a desiccator for 24 h before sampling. Prior to measurement, the flow rate of the $PM_{2.5}$ sampler was calibrated. Blank filters were collected and used to subtract the positive artifact caused by gas absorption. From 1 January to 31 January 2010, 31 quartz-filter samples and three blank samples were collected every 23.5 h (starting at 1000 LST each day and ending at 0930 LST the following day). The collected filter samples were stored in a freezer at −20°C to prevent the volatilization of particles.

A ∼0.5-cm^2 punch from the filter was analyzed for eight carbon fractions following the IMPROVE_A thermal/optical reflectance (TOR) protocol using a DRI model 2001 carbon analyzer (Atmoslytic, Inc., Calabasas, CA, USA; Cao et al., 2003, 2007; Chow et al., 2007). This produced four organic carbon (OC) fractions (OC1, OC2, OC3, and OC4 at 140°C, 280°C, 480°C, and 580°C, respectively, in a helium [He] atmosphere); OP (a pyrolyzed carbon fraction determined when transmitted laser light attained its original intensity after oxygen [O_2] was added to the analysis atmosphere); and three elemental carbon (EC) fractions (EC1, EC2, and EC3 at 580°C, 740°C, and 840°C, respectively, in a 2% O_2/98% He atmosphere). IMPROVE_TOR OC was operationally defined as OC1 + OC2 + OC3 + OC4 + OP, and EC was defined as EC1 + EC2 + EC3 − OP (Chow et al., 2007). Interlaboratory comparisons of samples using the IMPROVE_TOR protocol with samples using the TMO (thermal manganese dioxide oxidation) approach showed a difference of <5% for TC and <10% for OC and EC (Chow et al., 2007). Average field blanks were 2.04 and 0.12 μg m^{-3} for OC and EC, respectively.

One-fourth of each filter sample was used to determine the water-soluble ion mass concentrations. Four anions [sulfates (SO_4^{2-}), nitrates (NO_3^-), chlorides (Cl^-), and fluorides (F^-)] and five cations [sodium (Na^+), ammonia (NH_4^+), potassium (K^+), magnesium (Mg^{2+}), and calcium (Ca^{2+})] in aqueous extracts of the filters were determined by an ion chromatography (Dionex Corp, Sunnyvale, CA, Model Dionex 600). To extract the water-soluble species from the quartz filters, each sample was put into a separate 20-mL vial containing 10 mL distilled, deionized water (with a resistivity of 18 MΩ), and was shaken first by an ultrasonic instrument (Xinzhi Incorporated, Ningbo, China, Model SB-3200DTS) for 60 min and then by mechanical shaker (Shuoguang Incorporated, Shanghai, China, Model SG-3024) for 1 h to completely extract the ionic compounds. The extracts were stored at 4°C in a precleaned tube before analysis. Cation (Na^+, NH_4^+, K^+, Mg^{2+}, and Ca^{2+}) concentrations were determined using a CS12A column (Dionex Corp, Sunnyvale, CA.) with 20 mmol L^{-1} methanesulfonic acid (MSA) eluent. Anions (SO_4^{2-}, NO_3^-, Cl^-, and F^-) were separated by an AS11-HC column (Dionex Corp, Sunnyvale, CA), using 20 mmol L^{-1} potassium hydroxide (KOH) as the eluent. The limits of detection were <0.05 mg L^{-1} for anions and cations. Standard reference materials produced by the National Research Center for Certified Reference Materials, China, were analyzed for quality assurance purposes. Blank values were subtracted from sample concentrations.

2.4 *Continuous observation of meteorological parameters*

Meteorological parameters, including visibility (VIS), wind direction, wind speed, RH, temperature (TEMP), and precipitation (PR), were measured every 30 min. Visibility was measured using a present weather detector (Vaisala Company, Helsinki, Finland, Model PWD22); wind direction and wind speed were recorded by the wind monitor (Vaisala Company, Helsinki, Finland, Model QMW110A); and ambient RH and temperature were measured by a RH/temperature probe (Vaisala Company, Helsinki, Finland, Model QMH102). Both meteorological instruments were mounted 3 m above the roof of the station (53 m above ground).

3. Results and discussion

3.1 $PM_{2.5}$ *mass concentration,* b_{ap} *and* b_{sp}

The chemical species concentrations of $PM_{2.5}$, b_{ap}, b_{sp}, and meteorological parameters were collected during January 2010 (Table 1). During periods of intensive air pollution, the average $PM_{2.5}$ mass concentrations were 103.3±50.1 μg m^{-3}, which was close to 103 μg m^{-3} measured in autumn by Andreae et al. (2008) but was distinctly higher than 60.1 μg m^{-3} measured in summer by Jung et al. (2009). The average b_{ap} and b_{sp} were 79.3±47.5 Mm^{-1} and 469.3±279.4 Mm^{-1}, respectively. The value of b_{ext} (i.e., $b_{ap} + b_{sp}$) was slightly higher than 509 Mm^{-1} measured in autumn by Andreae et al. (2008) and was distinctly higher than 419 Mm^{-1} measured in summer by Jung et al. (2009). For the sample period, the weather conditions were categorized into four types: overcast, overcast rain, mostly sunny with haze, and overcast haze. The average mass concentrations of $PM_{2.5}$ were 122.7±37.4 μg m^{-3} and 127.6±44.4 μg m^{-3}, respectively, during periods that were mostly sunny with haze and periods of overcast haze that were obviously higher than those during overcast, and overcast rain periods. During overcast rain days, the $PM_{2.5}$ average concentration was slightly elevated and reached 61.1±36.8 μg m^{-3}. This concentration may have been due to low precipitation and shorter rainfall periods, which limited the scavenging efficiency of air pollutants. During overcast, $PM_{2.5}$ concentrations and the concentrations of chemical species were very low because the strong winds favored the dispersion of air pollutants. b_{ap} and b_{sp} during periods of haze were higher than during other periods due to higher $PM_{2.5}$ mass concentrations.

During the sampling period, two distinctly continuous periods of haze were recognized: (1) mostly sunny haze (from 12 January to 20 January) and (2) overcast haze (from 26 January to 31 January). Like Fig. 2 and Fig. 3 show that surface and 500-m-height wind directions changed from dry northerly winds to moist southerly winds during the two different periods of haze. As Fig. 4 show poor-visibility weather occurred on days with nearly calm winds and was closely related to higher RH and higher $PM_{2.5}$ mass concentrations. During the period of mostly sunny haze, visibility gradually decreased from 5.9 km to 2.1 km as RH increased from 39% to 78% and $PM_{2.5}$ mass concentration increased from 93.8 μg m^{-3} to 195.5 μg m^{-3}. Although $PM_{2.5}$ mass concentration reached an extreme value (195.5 μg m^{-3}) on 18 January 2010, the ($b_{ap} + b_{sp}$) maximum (1021 Mm^{-1}) and the visibility

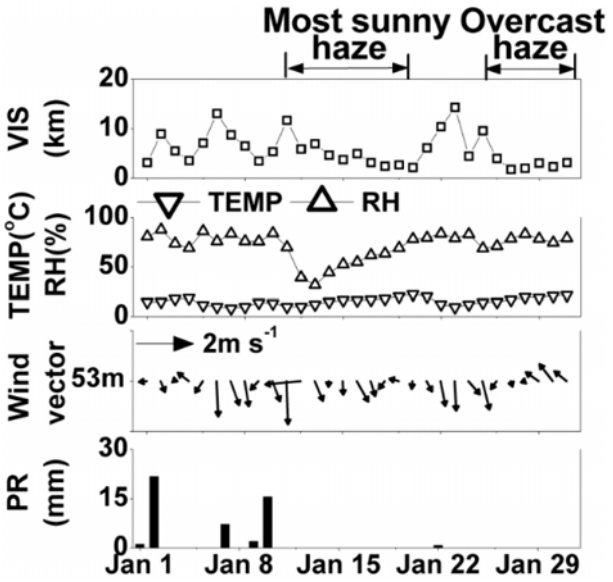

Fig. 2. Temporal variations of visibility and main meteorological parameters during the winter period.

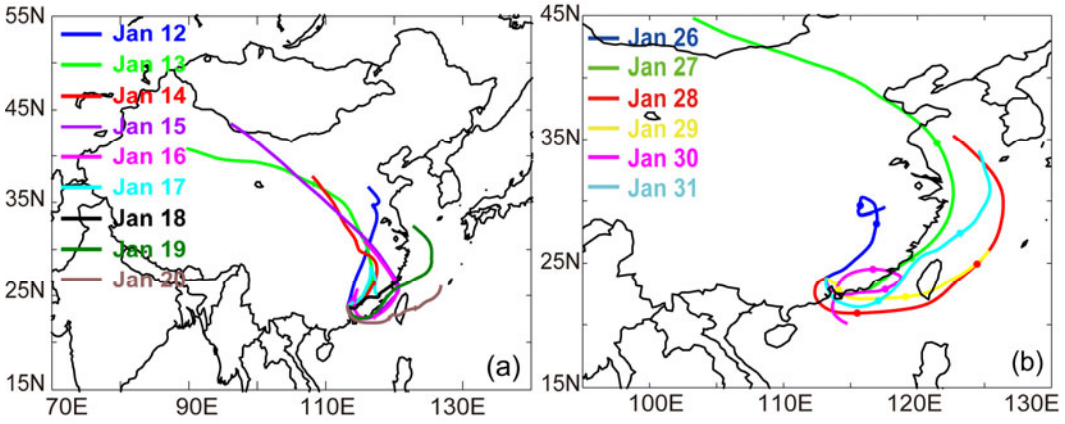

Fig. 3. Three days of backward trajectories terminating at SCIES site in Guangzhou during (a) the period of mostly sunny haze and (b) overcast haze.

Table1. The chemical species concentrations of $PM_{2.5}$ and light extinction coefficients and meteorological parameters in different weather condition at Guangzhou urban area in January 2010.

Weather condition	$PM_{2.5}$ ($\mu g\ m^{-3}$)	SO_4^{2-} ($\mu g\ m^{-3}$)	NO_3^- ($\mu g\ m^{-3}$)	Cl^- ($\mu g\ m^{-3}$)	Na^+ ($\mu g\ m^{-3}$)	NH_4^+ ($\mu g\ m^{-3}$)	K^+ ($\mu g\ m^{-3}$)	Ca^{2+} ($\mu g\ m^{-3}$)	OC ($\mu g\ m^{-3}$)	EC ($\mu g\ m^{-3}$)	b_{ap} (Mm^{-1})	b_{sp} (Mm^{-1})	TEMP (°C)	RH (%)	WS ($m\ s^{-1}$)
Overcast (n=4)	37.4±7.5	7.8±3.1	3.9±0.5	0.7±0.2	1.5±0.2	2.1±0.9	0.4±0.1	0.2±0.1	3.9±0.3	2.8±0.4	25.2±3.9	135.7±42.9	10.9±2.3	73.1±5.0	1.8±0.3
Overcast Rain (n=5)	61.1±36.8	10.5±7.3	6.2±4.6	2.1±1.4	1.9±0.6	3.4±2.8	0.8±0.7	0.2±0.1	7.1±4.0	4.7±2.5	47.9±27.1	235.2±166.6	12.8±2.8	83.8±2.5	0.9±0.4
Most sunny Haze (n=12)	122.7±37.4	21.7±5.7	17.8±5.3	2.9±1.7	2.3±0.4	7.6±2.1	1.2±0.4	0.8±0.5	15.0±7.2	8.8±3.3	86.0±33.7	519.5±188.6	15.5±3.3	59.0±14.8	0.8±0.5
Overcast Haze (n=10)	127.6±44.4	20.8±6.6	14.2±5.4	5.5±3.1	2.3±0.4	8.5±3.2	1.2±0.5	0.6±0.3	13.5±6.9	10.3±4.7	108.7±54.2	659.5±283.6	17.8±3.9	79.0±4.4	0.6±0.3
Average (n=31)	103.3±50.1	17.8±8.0	13.0±7.1	3.3±2.7	2.1±0.5	6.5±3.4	1.0±0.5	0.6±0.4	11.8±7.3	7.8±4.3	79.3±47.5	469.3±279.4	15.2±4.0	71.3±14.0	0.8±0.5

Note: n denotes sample number.

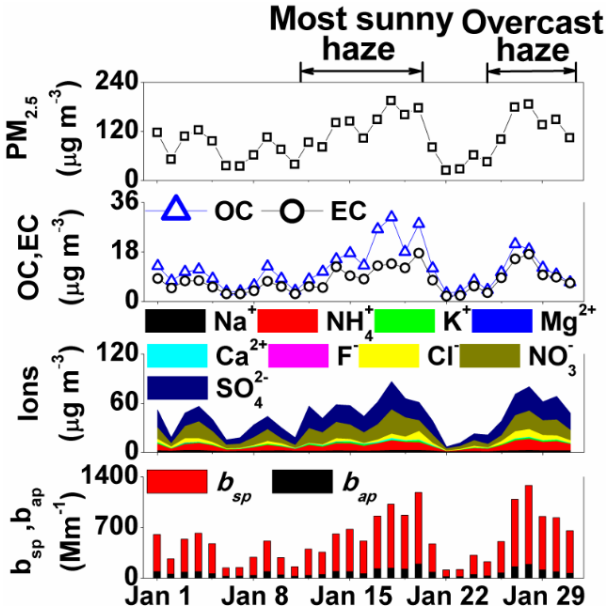

Fig. 4. Temporal variations of $PM_{2.5}$ and its chemical species, b_{ap} and b_{sp} during the winter period.

higher $PM_{2.5}$ mass concentration was due to higher RH, which enhanced the extinction efficiency of particles (Tie and Cao, 2009).

As cold northern air arrived on 21 January 2010, air temperature decreased, wind speed increased, and minimum (2.1 km) occurred on 20 January 2010. The the $PM_{2.5}$ concentration decreased until 24 January 2010. When the effect of cold northern air abated, wind decreased due to a uniform pressure field and pollutants accumulated, resulting in the period of overcast haze. During the first 3 days, the $PM_{2.5}$ mass concentration increased and reached an extreme value (186.8 μg m^{-3}) on 28 January 2010. At the same time b_{ap} and b_{sp} increased from 507 Mm^{-1} to 1283 Mm^{-1} and visibility decreased from 4.0 km to 2.0 km. As winds increased gradually thereafter, $PM_{2.5}$ mass concentrations decreased slightly, but visibility remained low. This can be attributed to the high level of RH that remained, which enhanced the extinction efficiencies of particles. Therefore, the days of severe haze occurred during conditions of calm wind, higher RH, and higher $PM_{2.5}$ mass concentrations.

3.2 *Reconstruction of b_{ap} and b_{sp} using the IMPROVE formula*

A formula developed for the IMPROVE program was applied to reconstruct the b_{ap} and b_{sp} by the $PM_{2.5}$ chemical composition (Pitchford et al., 2007). The IMPROVE formula can be simplified as follows:

$$b_{ap} = 10 \times [\mathrm{EC}]\,, \tag{1}$$

$$\begin{aligned} b_{sp} = {} & 2.2 \times f_S \times [\text{Small } (NH_4)_2SO_4] + \\ & 4.8 \times f_L \times [\text{Large } (NH_4)_2SO_4] + \\ & 2.4 \times f_S \times [\text{Small } NH_4NO_3] + \\ & 5.1 \times f_L \times [\text{Large } NH_4NO_3] + \\ & 2.8 \times [\text{Small OM}] + 6.1 \times [\text{Large OM}] + \\ & 1.7 \times f_{SS} \times [\mathrm{SS}] + 1 \times [\mathrm{FS}] + 0.6 \times [\mathrm{CM}]\,, \end{aligned} \tag{2}$$

$$[\text{Large X}] = [\text{Total X}]^2/20, [\text{Total X}] < 20\,, \tag{3}$$

$$[\text{Large X}] = [\text{Total X}], [\text{Total X}] \geqslant 20\,, \tag{4}$$

$$[\text{Small X}] = [\text{Total X}] - [\text{Large X}]\,, \tag{5}$$

where ammonium sulfate $[(NH_4)_2SO_4] = 1.375[SO_4^{2-}]$; ammonium nitrate $[NH_4NO_3]$ =1.29 nitrate $[NO_3^-]$; organic matter [OM] = 1.7 organic carbon [OC]; sea salt [SS] = 1.8 chlorine $[Cl^-]$; fine soil [FS] = 2.20 aluminum [Al] +2.49 silicone [Si] +1.94 titanium [Ti] + 1.63 calcium [Ca] + 2.42 iron [Fe]; coarse mass [CM] = $[PM_{10}] - [PM_{2.5}]$; and X = sulfates, nitrates, and OM mass concentrations, respectively. The units of b_{ap} and b_{sp} are given in Mm^{-1}. Mass concentrations are given in units of μg m^{-3}. The large mode represents aged particles, whereas the small mode represents freshly formed particles. These size modes are described by log-normal mass-size distributions with D_g and geometric standard deviations (σ_g) of 0.2 μm and 2.2 μm for the small mode and 0.5 μm and 1.5 μm for the large mode, respectively (Pitchford et al., 2007). RH growth curves of f_S, f_L, and f_{SS} of sulfates, nitrates, and SS refer to the work of Pitchford et al. (2007), which is suitable for application to the urban aerosol in Guangzhou (Jung et al., 2009). In this study, RH data was obtained from an inner RH detector inside a nephelometer rather than an ambient RH detector (i.e., precision reached 0.1%).

We excluded CM fraction for calculating b_{sp} because it made little contribution to b_{sp} (Cheung et al., 2005; Jung et al., 2009). As lack of elements of $PM_{2.5}$, we ignored contribution by FS fraction to b_{sp}. Although we ignored the CM and FS fractions, the measured b_{ap} and b_{sp} significantly correlated with reconstructed b_{ap} and b_{sp} calculated using the IMPROVE formula, respectively (see Figs. 5a, and b).

Strong correlations between measured b_{ap} and b_{sp} and reconstructed b_{ap} and b_{sp} were found to have R^2 = 0.95 and R^2 = 0.96, respectively. Furthermore, the slopes between measured b_{ap}, b_{sp} and reconstructed b_{ap}, b_{sp} were much closer to 1.0. Our results show that the IMPROVE formula can reflect the atmospheric extinction coefficient in Guangzhou urban area, when the

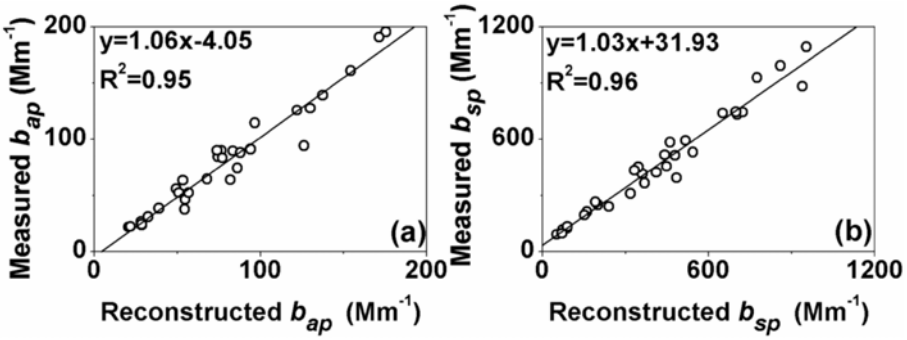

Fig. 5. Scatter plots of measured $b_{\rm ap}$ and $b_{\rm sp}$ versus reconstructed $b_{\rm ap}$ and $b_{\rm sp}$ and $b'_{\rm sp}$.

RH is $\leqslant$70%.

A revised IMPROVE formula was established for the Guangzhou urban area during the summer period by Jung et al. (2009). The localized parameterization formula can be written as follows:

$$b'_{\rm ap} = 7.7 \times [{\rm EC}]\,, \tag{6}$$

$$\begin{aligned} b'_{\rm sp} = {} & 2.2 \times f_{\rm S} \times [\text{Small } (NH_4)_2SO_4] + \\ & 3.24 \times f_{\rm L} \times [\text{Large } (NH_4)_2SO_4] + \\ & 2.4 \times f_{\rm S} \times [\text{Small } NH_4NO_3] + \\ & 4.47 \times f_{\rm L} \times [\text{Large } NH_4NO_3] + \\ & 2.8 \times [\text{Small OM}] + 4.93 \times [\text{Large OM}] + \\ & 1.7 \times f_{\rm SS} \times [\text{SS}] + 1 \times [PM_{2.5}\text{\_other}] + \\ & 0.6 \times [\text{CM}]\,, \end{aligned} \tag{7}$$

where $[PM_{2.5}\text{\_other}] = [PM_{2.5}] - 1.375[SO_4^{2-}] - 1.29[NO_3^-] - 1.7[OC] - [EC]$. According to the modified $b'_{\rm ap}$ and $b'_{\rm sp}$ formula, the correlation coefficient between the calculated $b'_{\rm ap}$, $b'_{\rm sp}$ and measured $b_{\rm ap}$, $b_{\rm sp}$ were slightly enhanced (see Figs. 6a and b). Comparing calculated $b'_{\rm ap}$ and $b'_{\rm sp}$ with calculated $b_{\rm ap}$ and $b_{\rm sp}$, calculated $b'_{\rm ap}$ and $b'_{\rm sp}$ were distinctly underestimated compared to the measured $b_{\rm ap}$ and $b_{\rm sp}$. This difference was apparently due to the mass scattering efficiency of sulfate; nitrate and OM concentrations for the large mode of fine particles were slightly lower than those calculated using the IMPROVE formula. These results prove that the IMPROVE formula and the localized parameterization of the modified IMPROVE formula can reflect the real atmospheric extinction coefficients in Guangzhou urban area when RH is <70%.

To investigate the applicability of the IMPROVE formula in the Guangzhou urban area under ambient RH, we used the visibility data obtained using the present weather detector (PWD). The visibility measurement was converted into a $b_{\rm ext}$ using a transfer function (Eq. 8) defined with an accurate transmissometer (Vaisala MITRAS, wavelength 550 nm).

$$b_{\rm ext} = 3000/{\rm VIS}\,, \tag{8}$$

where $b_{\rm ext}$ and VIS units in Mm^{-1} and km, respectively. Because visibility can be reduced by natural obstructions such as precipitation and RH >90%, we excluded visibility hourly data during periods of rainfall.

The $b_{\rm ext}$ includes the contributions from $b_{\rm sp}$ and gases ($b_{\rm sg}$) as well as $b_{\rm ap}$ and gases ($b_{\rm ag}$):

$$b_{\rm ext} = b_{\rm sp} + b_{\rm sg} + b_{\rm ap} + b_{\rm ag}\,. \tag{9}$$

Nitrogen dioxide (NO_2) is pollutant gas in the atmosphere that can absorb visible light. Absorption by NO_2 at a wavelength of 550 nm is computed using $b_{\rm ag}$

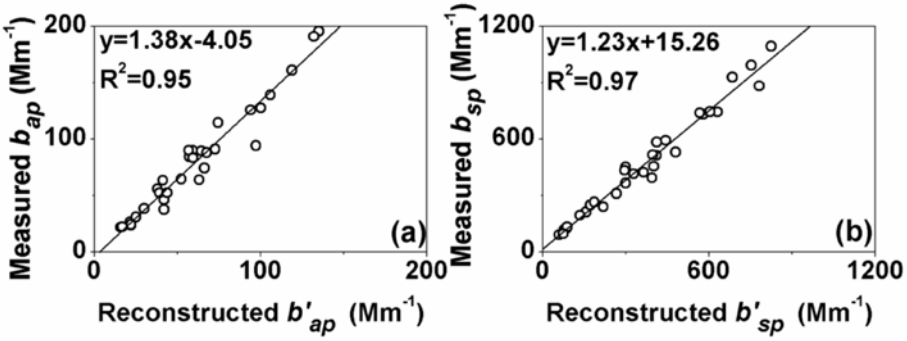

Fig. 6. Scatter plots of measured $b_{\rm ap}$ and $b_{\rm sp}$ versus reconstructed b'$_{\rm ap}$ and $b'_{\rm sp}$.

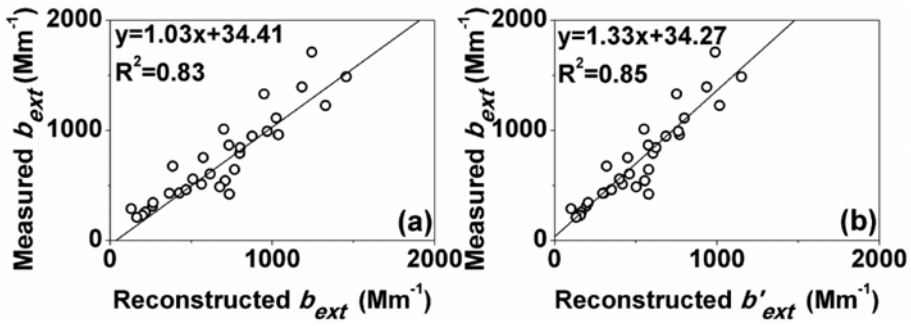

Fig. 7. Scatter plots of measured $b_{\rm ext}$ versus reconstructed $b_{\rm ext}$ and $b'_{\rm ext}$.

$= 330\times$ [NO_2], where the units of $b_{\rm ag}$ are Mm^{-1} and the units of NO_2 are ppm. $b_{\rm sg}$ is Rayleigh scattering. We excluded $b_{\rm sg}$ because it contributed little to $b_{\rm ext}$, which can be calculated as follows:

$$b_{\rm ext} = b'_{\rm sp} + b_{\rm ap} + b_{\rm ag} \ , \qquad (10)$$

where $b_{\rm ext}$ was calculated using the IMPROVE formula and the revised local IMPROVE formula with $PM_{2.5}$ chemical species and ambient RH.

Comparing the measured $b_{\rm ext}$ from PWD with calculated $b_{\rm ext}$ from the IMPROVE formula and calculated $b'_{\rm ext}$ from the localized parameterization-modified IMPROVE formula, the correlation coefficient between the measured $b_{\rm ext}$ and calculated $b'_{\rm ext}$ was slightly enhanced, but the slope of between the measured $b_{\rm ext}$ and the calculated $b_{\rm ext}$ was distinctly close to 1.00 (see Figs. 7a and b). These results suggest that the localized, parameterization-modified IMPROVE formula established by Jung et al. (2009) during summer period underestimated real atmospheric extinction coefficient in Guangzhou urban area during the winter period.

The atmospheric extinction coefficient calculated using the IMPROVE formula can reflect atmospheric extinction coefficient when RH is <70%, and the IMPROVE formula can also reflect the real atmospheric extinction coefficient in the Guangzhou urban area during the winter period.

3.3 *Source apportionment of light extinction coefficients*

Daily values of $b_{\rm ext}$ were calculated using the IMPROVE formula (Fig. 8). During periods of mostly sunny haze and overcast haze, the $b_{\rm ext}$ maximum values were 1328 Mm^{-1} and 1454 Mm^{-1}, respectively. The dominant species for $b_{\rm ext}$ were $(NH_4)_2SO_4$, NH_4NO_3, OM, and EC; in particular, $(NH_4)_2SO_4$ and NH_4NO_3 increase and their scattering efficiencies were enhanced when RH was >40%.

Figure 9 show the relative contribution to $b_{\rm ext}$ of atmospheric extinction compositions in different weather conditions. In this analysis, $(NH_4)_2SO_4$ made the largest contribution to the $b_{\rm ext}$, accounting for 35.0%, followed by NH_4NO_3 (22.9%), OM (16.1%),

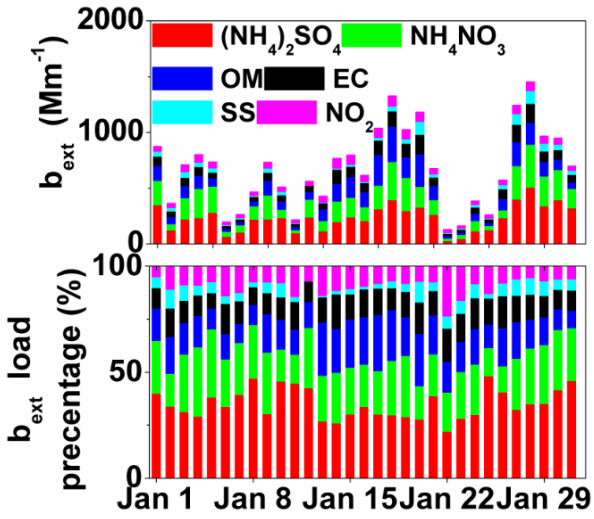

Fig. 8. Temporal variations of reconstructed $b_{\rm ext}$ and $b_{\rm ext}$ load percentages during the winter period.

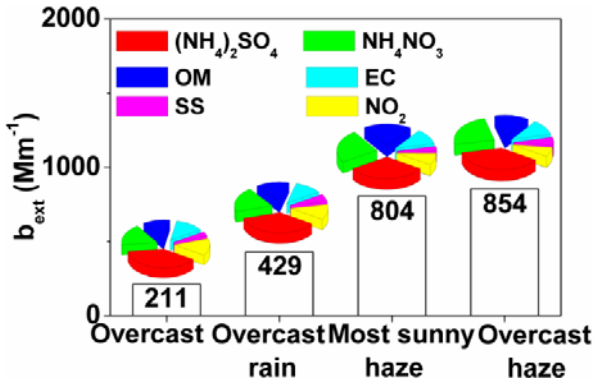

Fig. 9. Reconstructed $b_{\rm ext}$ and $b_{\rm ext}$ load percentages in different weather conditions during the winter period.

EC (11.8%), SS (4.7%), and NO_2 (9.6%) in all days. Combined, $(NH_4)_2SO_4$, NH_4NO_3, OM, EC, and NO_2 contributed >90% to b_{ext} during the winter period. Although the sulfate concentrations were almost equal during periods of mostly sunny haze and overcast haze, its relative contribution to b_{ext} was significant different due to higher RH during the overcast haze period that enhanced the scattering efficiency of sulfates. While the relative contribution of OM to b_{ext} during periods of mostly sunny haze was significantly higher than during periods of overcast haze, OM concentrations may be associated with more secondary organic aerosols produced by photochemical reaction.

4. Conclusions

From these intensive observations during January 2010, the characterizations of atmospheric visibility and its impact factors were determined for the Guangzhou urban area. The measured b_{ap} and b_{sp} values were 79.3±47.5 Mm^{-1}, 469.3±279.4 Mm^{-1} respectively, during the winter period. The two different haze periods showed a significant correlation with higher $PM_{2.5}$ concentrations and RH. When RH was <70%, the measured b_{ap} and b_{sp} had a significant correlation (R^2>0.95) with reconstructed b_{ap} and b_{sp} calculated using the IMPROVE formula. The measured b_{ext} had good correlation (R^2 >0.83) with calculated b_{ext} under ambient RH conditions. Our results show that the IMPROVE formula can reflect real atmospheric extinction coefficient in the Guangzhou urban area during the winter period. Using the IMPROVE formula, $(NH_4)_2SO_4$ was the largest contributor to b_{ext}, accounting for 35.0%, followed by NH_4NO_3 (22.9%), OM (16.1%), EC (11.8%), SS (4.7%), and NO_2 (9.6%). Therefore, based on this investigation, to improve the visibility in Guangzhou, urban environmental management steps should be taken to effectively control secondary and carbonaceous aerosol particles.

Acknowledgements. This study was supported by the Special Scientific Research Funds for Environment Protection Commonweal Section (Grant Nos. 200809143 and 201009001), Knowledge Innovation Program of the Chinese Academy of Sciences (Grant No. IAP09320). The authors would like to express their sincere appreciation for its financial support to accomplish this study. We also thank the anonymous reviewers for helpful comments and corrections on the manuscript.

REFERENCES

Andreae, M. O., O. Schmid, H. Yang, D. L. Chan, J. Z. Yu, L. M. Zeng, and Y. H. Zhang, 2008: Optical properties and chemical composition of the atmospheric aerosol in urban Guangzhou, China. *Atmos. Environ.*, **42**, 6335–6350.

Cao, J. J., and Coauthors, 2003: Characteristics of carbonaceous aerosol in Pearl River Delta Region, China during 2001 winter period. *Atmos. Environ.*, **37**, 1451–1460.

Cao, J. J., and Coauthors, 2007: Spatial and seasonal distributions of carbonaceous aerosols over China. *J. Geophys. Res.*, **112**, D22S11, doi: 10.1029/2006JD008205.

Chan, Y. C., R. W. Simpson, G. H. Mctainsh, P. D. Vowles, D. D. Cohen, and G. M. Bailey, 1999: Source apportionment of visibility degradation problems in Brisbane (Australia) using the multiple linear regression techniques. *Atmos. Environ.*, **33**, 3237–3250.

Cheng, Y. F., and Coauthors, 2008: Aerosol optical properties and related chemical apportionment at Xinken in Pearl River Delta of China. *Atmos. Environ.*, **42**, 6351–6372.

Cheung, H. C., T. Wang, K. Baumann, and H. Guo, 2005: Influence of regional pollution outflow on the concentrations of fine particulate matter and visibility in the coastal area of southern China. *Atmos. Environ.*, **39**, 6463–6474.

Chow, J. C., J. G. Watson, L. W. Chen, M. C. Chang, N. F. Robinson, D. Trimble, and S. Kohl. 2007: The IMPROVE_A temperature protocol for thermal/optical carbon analysis: maintaining consistency with a long-term database. *Journal of the Air & Waste Management Association*, **57**, 1014–1023.

Deng, X. J., and Coauthors, 2008: Long-term trend of visibility and its characterizations in the Pearl River Delta (PRD) region, China. *Atmos. Environ.*, **42**, 1424–1435.

Jung, J. S., Lee H. L., Kim Y. J., X. G. Liu, Y. H. Zhang, J. W. Gu, and S. J. Fan, 2009: Aerosol chemistry and the effect of aerosol water content on visibility impairment and radiative forcing in Guangzhou during the 2006 Pearl River Delta campaign. *Journal of Environmental Management*, **90**, 3231–3244.

Liu, X. G., and Coauthors, 2008: Influences of relative humidity and particle chemical composition on aerosol scattering properties during the 2006 PRD campaign. *Atmos. Environ.*, **42**, 1525–1536.

Malm, W. C., and D. E. Day, 2001: Estimates of aerosol species scattering characteristics as a function of relative humidity. *Atmos. Environ.*, **35**, 2845–2860.

Malm, W. C., J. F. Sisler, D. Huffman, R. A. Eldred, and T. A. Cahill, 1994: Spatial and seasonal trends in particle concentration and optical extinction in the United States. *J. Geophys. Res.*, **99**(D1), 1347–1370.

Pitchford, M. L., W. C. Malm, B. A. Schichtel, N. Kumar, D. H. Lowenthal, and J. L. Hand, 2007: Revised formula for estimating light extinction from IMPROVE particle speciation data. *Journal of the Air & Waste Management Association*, **57**, 1326–1336.

Tan, J. H., and Coauthors, 2009: Chemical characteristics of haze during summer and winter in Guangzhou. *Atmospheric Research*, **94**, 238–245.

Tao, J., K. F. Ho, L. G. Chen, L. H. Zhu, J. L. Han, and Z. C. Xu, 2009: Effect of chemical composition of $PM_{2.5}$ on visibility in Guangzhou, China, 2007 spring. *Particuology*, **7**(1), 68–75.

Tie, X. X., and J. J. Cao, 2009: Aerosol pollution in China: Present and future impact on environment. *Particuology*, **7**, 426–431.

Watson, J. G., 2002: Visibility: Science and Regulation. *Journal of the Air & Waste Management Association*, **52**, 628–713.

Wu, D., and Coauthors, 2009: Black carbon aerosols and their radiative properties in the Pearl River Delta region. *Science in China* (*D*), **52**(8), 1152–1163.

Wu, D., X. X. Tie, C. C. Li, Z. M. Ying, A. K. H. Lau, J. Huang, X. J. Deng, and X. Y. Bi, 2005: An extremely low visibility event over the Guangzhou region: A case study. *Atmos. Environ.*, **39**, 6568–6577.

Yan, P., J. Tang, J. Huang, J. T. Mao, X. J. Zhou, Q. Liu, Z. F. Wang, and H. G. Zhou, 2008: The measurement of aerosol optical properties at a rural site in Northern China. *Atmospheric Chemistry and Physics*, **8**, 2229–2242.

Yang, L. X., D. C. Wang, S. H. Cheng, Z. Wang, Y. Zhou, X. H. Zhou, and W. X. Wang, 2007: Influence of meteorological conditions and particulate matter on visual range impairment in Jinan, China. *Science of the Total Environment*, **383**, 164–173.